An Improved IEM2Mc Model for Surface Bistatic Scattering

Wenchao Zheng [1], Yi Leng [2], and Qingxia Li [1]

[1] Science and Technology on Multi-Spectral Information Processing Laboratory
School of Electronic Information and Communications
Huazhong University of Science and Technology, Wuhan, 430074, China
wenchaozheng@hust.edu.cn, qingxia_li@mail.hust.edu.cn

[2] Department of Information Counter
Air Force Early Warning Academy, Wuhan, 430019, China
lengyi119@aliyun.com (Corresponding author)

Abstract ─ In this paper, the IEM2Mc (integral equation model for second-order multiple s and complex-permittivity scattering media) model is modified in two aspects in bistatic scattering. Firstly, the full forms of the surface current terms in the Kirchhoff surface fields are reserved. Secondly, a transition function is used to estimate the Fresnel coefficients instead of the original expression. The simulating results of the improved IEM2Mc are compared with those of small perturbation method (SPM), Kirchhoff model (KA), and method of moment (MoM) for random rough surfaces scattering problems. It is shown that the improved IEM2Mc provides better predictions than the original form, especially for the large incident or scattering angle.

Index Terms ─ Bistatic scattering, IEM2M, IEM2Mc, KA, rough surface, SPM.

I. INTRODUCTION

IEM (integral equation model) is a widely used analytical model for the electromagnetic wave scattering in microwave remote sensing. The original IEM was proposed by Fung [1] based on the approximation for the integral equations described by Poggio and Miller. The further studies focus on removing the simplification in IEM to improve the accuracy. IEMM [2] comprises the multiple scattering effects by including the full form of the spectral representation of the Green's function (the effect of upward and downward waves on the surface fields). However, the IEMM doesn't handle the single scattering. Full form of the spectral representation of the gradient of the Green's function appears in the IEM2M model [3] and the advanced IEM model (AIEM) [4] for solving surface scattering problems.

However, both IEM2M and AIEM fail to deal with scattering from rough surface of complex-permittivity media. An error function related terms for the cross and complementary scattering coefficients are introduced by Du [5] to deal with scattering from rough surfaces of complex-permittivity media. Also, Alvarez-Perez [6] extends IEM2M to IEM2Mc for complex-permittivity scattering media based on a full 3D expansion of the outgoing spherical wave. Because of the full 3D expansion of the outgoing spherical wave, IEM2Mc in [6] is much simpler than the method in [5].

In the IEM2Mc, the expressions of the surface fields neglect the sum of horizontal and vertical Fresnel reflection coefficients. This neglection may bring about erroneous results at the bistatic configurations, particularly when the incident or scattering angle is large. Besides, in the emissivity calculations, this neglection may also produce unacceptable prediction, since the error will be accumulated by integrating all the scattering power over the half-space.

In this paper, the sum of horizontal and vertical Fresnel reflection coefficients in surface current expressions is added and a transition function is applied here to predict the Fresnel reflection. The newly derived IEM2Mc is verified by comparing the results with the SPM, KA, and MoM. The simulating is made on rough surfaces with small or moderate heights. In Section II, the scattered fields at the far zone, the scattered incoherent power and the scattering coefficients are specified. In Section III, the improved part of IEM2Mc is illustrated. Numerical simulations and comparisons with other methods are provided in Section IV. Finally, our conclusion is presented in Section V.

II. THE FORMULAS OF THE SCATTERING PROBLEM

Here we consider an incident plane wave impinging upon a rough surface from medium 1 to medium 2. The incident electric and magnetic fields

Submitted On: October 7, 2014
Accepted On: May 20, 2015

are:

$$\vec{E}^{\,i} = \hat{p}\, E_0 \exp[i(\vec{k}_1 \cdot \vec{r})] = \hat{p}\, E^i, \tag{1}$$

$$\vec{H}^{\,i} = \hat{k}_i \times (\hat{p}\, E^i)/\eta_1, \tag{2}$$

where $\hat{p}$ is the unit polarization vector; $\hat{k}_i$ is the unit vector in the incident direction; E_0 is the amplitude of the electric field; η_1 is the intrinsic impedance of medium 1; $\vec{k}_1 = \hat{k}_i k$, k is the wave number.

The equations for the surface tangential fields are:

$$\begin{aligned}\hat{n}'\times\vec{E}' &= 2\hat{n}'\times\vec{E}^{\,i} + \frac{1}{2\pi}\hat{n}'\times\int[ik\eta_1(\hat{n}''\times\vec{H}'')G_1 \\ &+ (\hat{n}''\times\vec{E}'')\times\nabla'' G_1 + (\hat{n}''\cdot\vec{E}'')\nabla'' G_1]ds'',\end{aligned} \tag{3}$$

$$\begin{aligned}\hat{n}'\times\vec{H}' &= 2\hat{n}'\times\vec{H}^{\,i} + \frac{1}{2\pi}\hat{n}'\times\int[-\frac{ik}{\eta_1}(\hat{n}''\times\vec{E}'')G_1 \\ &+ (\hat{n}''\times\vec{H}'')\times\nabla'' G_1 + (\hat{n}''\cdot\vec{H}'')\nabla'' G_1]ds'',\end{aligned} \tag{4}$$

where k $k = \omega\sqrt{\varepsilon_1\mu_1}$; G_1 is the Green function in medium 1; η_1 is the intrinsic impedance of medium 1; $\hat{n}'$ and $\hat{n}''$ are the unit normal vectors to the surface; $\hat{n}'\times\vec{E}'$ and $\hat{n}'\times\vec{H}'$ are the total tangential fields on surface in medium 1.

In IEM2Mc, a full 3D spectrum of the Green function is used instead of the Weyl representation of the Green function. The corresponding expression can be written as:

$$\begin{aligned}&G_m(\vec{r}',\vec{r}'') = \\ &\frac{1}{2\pi^2}\iiint_{R^3} e^{i[u(x'-x'')+v(y'-y'')]}\frac{e^{iw(z'-z'')}}{(w-q_m)(w+q_m)}dudvdw, \\ &q_m = \begin{cases}(k_m^2-u^2-v^2)^{1/2} & ,k_m^2 \ge u^2+v^2 \\ i(u^2+v^2-k_m^2)^{1/2} & ,k_m^2 \le u^2+v^2\end{cases}.\end{aligned} \tag{5}$$

The gradient of the Green function is given by:

$$\begin{aligned}&\nabla'' G_m(\vec{r}',\vec{r}'') = \frac{1}{2i\pi^2}\times \\ &\iiint_{R^3} e^{i[u(x'-x'')+v(y'-y'')+w(z'-z'')]}\frac{e^{iw(z'-z'')}}{(w-q_m)(w+q_m)}\vec{g}_m dudvdw, \\ &\vec{g}_m = u\hat{x}+v\hat{y}+w\hat{z}, \\ &m = \begin{cases}1, \ in \ \ medium\,1 \\ 2, \ in \ \ medium\,2\end{cases}.\end{aligned} \tag{6}$$

Because of the full 3D spectrum of the Green function, the damped waves originating inside a lossy medium or the evanescent waves in non-lossy medium can be evaluated.

The far-zone scattered fields are calculated in terms of surface fields. The far-zone scattered fields in the medium above the rough surface are derived according to the Stratton-Chu integral. It is divided into the Kirchhoff field and the complementary field:

$$E_{qp}^s = (E_{qp}^s)_k + (E_{qp}^s)_c. \tag{7}$$

In equation (7), the incident polarization is denoted by p and the receiving polarization by q. The incident polarization (p) could be horizontal polarization (h) or vertical polarization (v), and so is the receiving polarization (q):

$$\begin{aligned}E_{qp}^s = K\int_s[&(\hat{q}_s\times\hat{k}^s)\cdot(\hat{n}'\times\vec{E}_p'\,) + \eta_1\hat{q}_s\cdot(\hat{n}'\times\vec{H}_p'\,)]\times \\ &e^{-i\vec{k}^s\cdot\vec{r}'}D'dx'dy',\end{aligned} \tag{8}$$

where $K = ik_1 e^{ik_1R}/(4\pi R)$; $D' = \sqrt{1+Z_{x'}^2+Z_{y'}^2}$; $\hat{q}_s$ is the polarization vector.

The expression of the Kirchhoff field is:

$$(E_{qp}^s)_k = KE_0\int_s f_{qp}e^{-i[(\vec{k}^s-\vec{k}^i)\cdot\vec{r}']}dx'dy', \tag{9}$$

$$\begin{aligned}f_{qp} = D'[&(\hat{q}\times\hat{k}^s)\cdot(\hat{n}'\times\vec{E}_p'\,)_k \\ &+ \eta_1\hat{q}\cdot(\hat{n}'\times\vec{H}_p'\,)_k]/E^i.\end{aligned} \tag{10}$$

The Kirchhoff components will not be affected by the introduction of the full 3D Green function. The complementary field can be obtained in conjunction with a spectral representation for the Green's function and its gradient:

$$\begin{aligned}(E_{qp}^s)_c &= K\int_s[(\hat{q}_s\times\hat{k}^s)\cdot(\hat{n}'\times\vec{E}_p'\,)_c + \eta_1\hat{q}_s\cdot(\hat{n}'\times\vec{H}_p'\,)_c]\times \\ &\quad e^{-i\vec{k}^s\cdot\vec{r}'}D'dx'dy' \\ &= \frac{KE_0}{8\pi^3}\{\int_{R^3}\int_{S^2}F_{qp}^1(\vec{k}^{\,i},\vec{k}^{\,s})\frac{e^{i[u(x'-x'')+v(y'-y'')+w(z'-z'')]}}{(w-q_1)(w+q_1)}\times \\ &\quad e^{-i\vec{k}^s\cdot\vec{r}'}e^{i\vec{k}^i\cdot\vec{r}''}dx'dy'dx''dy''dudvdw + \\ &\quad \int_{R^3}\int_{S^2}F_{qp}^2(\vec{k}^{\,i},\vec{k}^{\,s})\frac{e^{i[u(x'-x'')+v(y'-y'')+w(z'-z'')]}}{(w-q_2)(w+q_2)}\times \\ &\quad e^{-i\vec{k}^s\cdot\vec{r}'}e^{i\vec{k}^i\cdot\vec{r}''}dx'dy'dx''dy''dudvdw\},\end{aligned} \tag{11}$$

$$F_{qp}^m = D'[(\hat{q}\times\hat{k}^s)\cdot(\hat{n}'\times\vec{E}_p'\,)_c^m + \eta_1\hat{q}\cdot(\hat{n}'\times\vec{H}_p'\,)_c^m]. \tag{12}$$

According to the new expression of the scattered field, the average incoherent power is obtained. In the original IEM2Mc, the Kirchhoff incoherent power is the same as that given in IEM2M. The cross incoherent power is:

$$\begin{aligned}S_{qp}^{kc} &= \mathrm{Re}\{1/\eta_1\}\,\mathrm{Re}\{\langle E_{qp}^{sc}E_{qp}^{sk*}\rangle - \langle E_{qp}^{sc}\rangle\langle E_{qp}^{sk*}\rangle\} \\ &= \frac{|KE_0|^2}{8\pi^2}\mathrm{Re}\{1/\eta_1\sum_{m=1,2}\mathrm{Re}\{f_{qp}^*\int_{R^3}dudvdw \\ &\quad \int_{S^3}dx'dy'dx''dy''dx'''dy''' \\ &\quad \times e^{i[u(x'-x'')+v(y'-y'')]}e^{-i[k_{sx}(x'-x''')+k_{sy}(y'-y''')]} \\ &\quad \times e^{i[k_x(x''-x''')+k_y(y''-y''')]} \\ &\quad \times[\langle e^{-ik_{sz}(z'-z''')}e^{ik_z(z''-z''')}e^{iw(z'-z'')}F_{qp}^m(\vec{k}^{\,i},\vec{k}^{\,s})\rangle \\ &\quad -\langle e^{-ik_{sz}z'}e^{ik_z z''}e^{iw(z'-z'')}F_{qp}^m(\vec{k}^{\,i},\vec{k}^{\,s})\rangle\langle e^{i(k_{sz}-k_z)z'''}\rangle]\},\end{aligned} \tag{13}$$

if $\xi = x'-x''', \varsigma = y'-y''', \xi' = x''-x''', \varsigma' = y''-y'''$, then

$$\begin{aligned} S_{qp}^{kc} &= \mathrm{Re}\{1/\eta_1\}\,\mathrm{Re}\{\langle E_{qp}^{sc} E_{qp}^{sk\,*}\rangle - \langle E_{qp}^{sc}\rangle\langle E_{qp}^{sk\,*}\rangle\} \\ &= \frac{|KE_0|^2}{8\pi^2}\mathrm{Re}\{1/\eta_1 \sum_{m=1,2}\sum_{r=-1,1}\mathrm{Re}\{f_{qp}^{*}\int_{R^3} dudvdw \\ &\int d\xi d\varsigma d\xi' d\varsigma' e^{i[u(\xi-\xi')+v(\varsigma-\varsigma')]} e^{-i[k_{sx}\xi+k_{sy}\varsigma]} e^{i[k_x\xi'+k_y\varsigma']} \\ &\times e^{-\sigma^2[(k_{sz}-w)(k_z-w)(1-\rho_{12})]} F_{qp}^{m}(\vec{k}^{\,i},\vec{k}^{\,s}) \\ &\times [e^{-\sigma^2[(k_{sz}-w)(k_{sz}-k_z)(1-\rho_{13})]} e^{-\sigma^2[(w-k_z)(k_{sz}-k_z)(1-\rho_{23})]} \\ &- e^{-\sigma^2(k_{sz}-k_z)^2}]\}, \end{aligned} \tag{14}$$

where

$$\rho_{12} = \rho(\xi-\xi',\varsigma-\varsigma'); \quad \rho_{13} = \rho(\xi,\varsigma); \quad \rho_{23} = \rho(\xi',\varsigma').$$

The corresponding scattering coefficient is:

$$\begin{aligned} (\sigma^0)_{qp}^{kc} &= \frac{k_1^2}{2}\sum_{m=1,2}\mathrm{Re}\{f_{qp}^{*} e^{-\sigma^2[k_{sx}^2+k_{sy}^2-k_{sz}k_z]}\int_{R^2} dudv \\ &\times F_{qp}^{m}(\vec{k}^{\,i},\vec{k}^{\,s})\; e^{-\sigma^2[w^2-(k_{sz}+k_z)w]}[\sum_{n=1}^{\infty}\frac{[-\sigma^2(k_{sz}-w)(k_z-k_{sz})]^n}{n!} \\ &\times W_1^{(n)}(k_{sx}-u,k_{sy}-v)\delta(u-k_x)\delta(v) \\ &+\sum_{l=1}^{\infty}\frac{[\sigma^2(k_z-w)(k_z-k_{sz})]^l}{l!}W_1^{(l)}(u-k_x,v)\delta(k_{sx}-u) \\ &\times\delta(k_{sy}-v)+\frac{1}{2\pi}\sum_{n=1}^{\infty}\frac{[-\sigma^2(k_{sz}-w)(k_z-k_{sz})]^n}{n!}\times \\ &\sum_{l=1}^{\infty}\frac{[\sigma^2(k_z-w)(k_z-k_{sz})]^l}{l!}W_1^{(n)}(k_{sx}-u,k_{sy}-v) \\ &\times W_1^{(l)}(u-k_x,v)]\}. \end{aligned} \tag{15}$$

$W^{(n)}(\cdot)$ is the Fourier transform of the nth power of the normalized surface correlation function.

The complementary incoherent power is:

$$\begin{aligned} S_{qp}^{c} &= \frac{1}{2}\mathrm{Re}\{1/\eta_1\}\,\mathrm{Re}\{\langle E_{qp}^{sc} E_{qp}^{sc\,*}\rangle - \langle E_{qp}^{sc}\rangle\langle E_{qp}^{sc\,*}\rangle\} \\ &= \frac{|KE_0|^2}{2^7\pi^4}\mathrm{Re}\{1/\eta_1\}\times\sum_{m,n=1,2}\{\int_{R^6} dudvdwdu'dv'dw' \\ &\int_{s^4} dx'dy'dx''dy''dx'''dy'''dx^{v}dy^{v} \\ &\times e^{i[u(x'-x'')-u'(x'''-x^{v})+v(y-y'')-v'(y'''-y^{v})]} e^{-i[k_{sx}(x'-x''')+k_{sy}(y'-y''')]} \\ &e^{i[k_x(x''-x^{v})+k_y(y''-y^{v})]}[\langle e^{-ik_{sz}(z'-z''')} e^{ik_z(z''-z^{v})} e^{iw(z'-z'')} \\ &\times e^{-iw(z'''-z^{v})} F_{qp}^{m}(\vec{k}^{\,i},\vec{k}^{\,s}) F_{qp}^{n*}(\vec{k}^{\,i},\vec{k}^{\,s})\rangle \\ &-\langle e^{-i(k_{sz}z'+k_z z'')} e^{iw(z'-z'')} F_{qp}^{m}(\vec{k}^{\,i},\vec{k}^{\,s})\rangle\times \\ &\langle e^{i(k_{sz}z'''-k_z z^{v})} e^{-iw(z'''-z^{v})} F_{qp}^{n*}(\vec{k}^{\,i},\vec{k}^{\,s})\rangle]\}. \end{aligned} \tag{16}$$

The scattering coefficient of the complementary term is:

$$\begin{aligned} (\sigma^0)_{qp}^{c} &= \frac{k_1^2}{16}\sum_{m,n=1,2}\{e^{-\sigma^2(k_{sz}^2+k_z^2)}\int_{R^4} dudvdu'dv' F_{qp}^{m}(\vec{k}^{\,i},\vec{k}^{\,s}) \\ &F_{qp}^{n*}(\vec{k}^{\,i},\vec{k}^{\,s})\, e^{-\sigma^2[w_m^2+w_n^2-(k_{sz}+k_z)(w_m+w_n)]}[\sum_{h=1}^{\infty}\frac{[-\sigma^2(k_{sz}-w_m)(w_n-k_{sz})]^h}{h!} \\ &W_1^{(h)}(k_{sx}-u,k_{sy}-v)\delta(u-k_x)\delta(v)\delta(u-u')\delta(v-v')+ \\ &\sum_{l=1}^{\infty}\frac{[-\sigma^2(k_{sz}-w_m)(k_z-w_n)]^l}{l!}W_1^{(l)}(k_{sx}-u,k_{sy}-v)\delta(u-k_x)\delta(v) \\ &\times\delta(k_{sx}-u')\delta(k_{sy}-v')+\sum_{n=1}^{\infty}\frac{[-\sigma^2(k_z-w_m)(k_{sz}-w_n)]^n}{n!} \\ &\times W_1^{(n)}(u-k_x,v-k_y)\delta(k_{sx}-u)\delta(k_{sy}-v)\delta(u'-k_x)\delta(v) \\ &+\sum_{t=1}^{\infty}\frac{[-\sigma^2(k_z-w_m)(w_n-k_z)]^t}{t!}W_1^{(t)}(u-k_x,v-k_y)\delta(k_{sx}-u) \\ &\times\delta(k_{sy}-v)\delta(u-u')\delta(v-v')+\frac{1}{2\pi}\sum_{h=1}^{\infty}\frac{[-\sigma^2(k_{sz}-w_m)(w_n-k_{sz})]^h}{h!} \\ &\sum_{t=1}^{\infty}\frac{[-\sigma^2(k_z-w_m)(w_n-k_z)]^t}{t!}\times W_1^{(h)}(k_{sx}-u,k_{sy}-v) \\ &\times W_1^{(t)}(u-k_x,v-k_y)\delta(u-u')\delta(v-v')+ \\ &\frac{1}{2\pi}\sum_{l=1}^{\infty}\frac{[-\sigma^2(k_{sz}-w_m)(k_z-w_n)]^l}{l!}\sum_{n=1}^{\infty}\frac{[-\sigma^2(k_z-w_m)(k_{sz}-w_n)]^n}{n!} \\ &W_1^{(l)}(k_{sx}-u,k_{sy}-v)\times W_1^{(n)}(u-k_x,v-k_y)\delta(u+u'-k_{sx}-k_x) \\ &\times\delta(v+v'-k_{sy})]\}. \end{aligned} \tag{17}$$

The scattering coefficients are obtained by:

$$\sigma^0 = (\sigma^0)_{qp}^{k} + (\sigma^0)_{qp}^{kc} + (\sigma^0)_{qp}^{c}. \tag{18}$$

A more compact form is written as follows by extracting the single-scattering terms out of the cross and complementary terms and putting them together along with the Kirchhoff term:

$$\begin{aligned} (\sigma^o)_{qp}^{s} &= \frac{1}{2}k_1^2 e^{-\sigma^2(k_{sz}-k_z)^2}\times \\ &\sum_{n=1}^{\infty}\frac{\sigma^{2n}}{n!}|I_{qp}^{(n)}|^2 W_1^{(n)}(k_{sx}-k_x,k_{sy}-k_y), \end{aligned} \tag{19}$$

where

$$\begin{aligned} &W_1^{(n)}(k_{sx}-k_x,k_{sy}-k_y) \\ &= \frac{1}{2\pi}\int d\xi d\varsigma\,\rho^n(\xi,\varsigma)e^{-i[(k_{sx}-k_x)\xi+(k_{sy}-k_y)\varsigma]}, \end{aligned} \tag{20}$$

$$I_{qp}^{(n)} = (k_{sz}-k_z)^n f_{qp} + \frac{1}{4}\sum_{m=1}^{2}\sum_{r=1}^{2}\sum_{t=1}^{4}\gamma_m^{r,t}, \tag{21}$$

$$\gamma_m^{r,t} = \Gamma_m^{r,t} F_{qp}^{m,r,t}(\vec{k}^{\,i},\vec{k}^{\,s}), \tag{22}$$

$$\begin{aligned} \Gamma_m^{r,t} &= (-1)^{r(n-t)}\exp\{-\sigma^2 k_{sz}k_z\} \\ &\times\begin{cases} I^{(n-1)}(k_{sz}+k_z,q_m,a), & \text{if } t=1 \\ I^{(n)}(k_{sz}+k_z,q_m,a), & \text{if } t=2 \\ I_w^{(n-1)}(k_{sz}+k_z,q_m,a), & \text{if } t=3 \\ I_w^{(n)}(k_{sz}+k_z,q_m,a), & \text{if } t=4 \end{cases}, \end{aligned} \tag{23}$$

$$a=\begin{cases}k_{sz}, \text{ if } r=1\\ k_z, \text{ if } r=2\end{cases}, \tag{24}$$

$$I_0(k,q,a)=\exp\{-\sigma^2 k(a-\frac{k}{4})\}\times \frac{1}{q}[w(\sigma(\frac{k}{2}+q))+w(\sigma(-\frac{k}{2}+q))], \tag{25}$$

$$I^{(n)}(k,q,a)=\int_{-\infty}^{\infty}dw\frac{\exp\{-\sigma^2(w^2-kw)\}}{w^2-q^2}(w-a)^n =\frac{\exp\{\sigma^2 ka\}}{\sigma^{2n}}\frac{d^n I_0(k,q,a)}{dk^n}, \tag{26}$$

$$I_w^{(n)}(k,q,a)=\int_{-\infty}^{\infty}dw\frac{\exp\{-\sigma^2(w^2-kw)\}}{w^2-q^2}w(w-a)^n =\frac{1}{\sigma^2}\frac{dI^{(n)}(k,q,a)}{dk}. \tag{27}$$

III. IMPROVED PARTS FOR IEM2MC

In this section, new surface field coefficients are derived by keeping the full forms of the surface current terms in the Kirchhoff surface fields. Then, the transition function is applied to predict the Fresnel coefficients.

A. Surface field coefficients

The estimates of surface fields are the sum of the Kirchhoff and complementary fields. They are related to the scattering coefficients by f_{qp} and F_{qp} coefficients. In the original IEM2Mc, the terms of the surface fields neglect the sum of horizontal and vertical Fresnel reflection coefficients. Here, in the improved IEM2Mc, the complete form of the surface fields are applied to calculate f_{qp}. The f_{qp} coefficients with the sum of horizontal and vertical Fresnel reflection coefficients [7] are:

$$\begin{aligned}f_{vv}=&-[(1-R_v)\hat{h}_s\cdot(\hat{n}'\times\hat{v})+(1+R_v)\hat{v}_s\cdot(\hat{n}'\times\hat{h})]D'\\&-(R_v+R_h)(\hat{v}\cdot\hat{t})[(\hat{h}_s\cdot\hat{d})(\hat{n}'\cdot\hat{k}_i)-(\hat{n}'\cdot\hat{d})(\hat{h}_s\cdot\hat{k}_i)\\&-(\hat{v}_s\cdot\hat{t})(\hat{n}'\cdot\hat{k}_i)]D',\end{aligned} \tag{28}$$

$$\begin{aligned}f_{vh}=&[(1-R_h)\hat{v}_s\cdot(\hat{n}'\times\hat{v})-(1+R_h)\hat{h}_s\cdot(\hat{n}'\times\hat{h})]D'\\&-(R_v+R_h)(\hat{h}\cdot\hat{d})[(\hat{h}_s\cdot\hat{t})(\hat{n}'\cdot\hat{k}_i)-(\hat{n}'\cdot\hat{d})(\hat{v}_s\cdot\hat{k}_i)\\&+(\hat{v}_s\cdot\hat{d})(\hat{n}'\cdot\hat{k}_i)]D',\end{aligned} \tag{29}$$

$$\begin{aligned}f_{hv}=&[(1-R_v)\hat{v}_s\cdot(\hat{n}'\times\hat{v})-(1+R_v)\hat{h}_s\cdot(\hat{n}'\times\hat{h})]D'\\&-(R_v+R_h)(\hat{v}\cdot\hat{t})[(\hat{h}_s\cdot\hat{t})(\hat{n}'\cdot\hat{k}_i)-(\hat{n}'\cdot\hat{d})(\hat{v}_s\cdot\hat{k}_i)\\&+(\hat{v}_s\cdot\hat{d})(\hat{n}'\cdot\hat{k}_i)]D',\end{aligned} \tag{30}$$

$$\begin{aligned}f_{hh}=&[(1+R_v)\hat{v}_s\cdot(\hat{n}'\times\hat{h})+(1-R_v)\hat{h}_s\cdot(\hat{n}'\times\hat{v})]D'\\&-(R_v+R_h)(\hat{h}\cdot\hat{d})[(\hat{h}_s\cdot\hat{d})(\hat{n}'\cdot\hat{k}_i)-(\hat{n}'\cdot\hat{d})(\hat{h}_s\cdot\hat{k}_i)\\&-(\hat{v}_s\cdot\hat{t})(\hat{n}'\cdot\hat{k}_i)]D'.\end{aligned} \tag{31}$$

Substituting Equations (28)-(31) into (21), we obtain the newly derived $I_{qp}^{(n)}$. This modification is made on the Kirchhoff field and there will be no change with the complementary fields.

B. Transition function

In IEM2Mc, the Fresnel coefficient is chosen with a posteriori method:

$$R\rightarrow(R(\theta)+R(\theta_s))/2. \tag{32}$$

This means an approximation to the first mean-value theorem for integration together with the imposition of reciprocity on the scattered fields [6]. This approximation seems to work well in the IEM2M and IEM2Mc. However, when the Rv+Rh term is considered, the equation (32) may not derive good results.

Here, the transition function which was reported in [8] is applied instead of the original expression. The transition function links the two extremes for the $R(\theta_i)$ (Fresnel reflection evaluated at incident angle) and $R(\theta_{sp})$ (Fresnel reflection evaluated at specular angle). Thus, the Fresnel coefficients could be determined by a transition function as:

$$R_p=R_p(\theta_i)+(R_p(\theta_{sp})-R_p(\theta_i))(1-\frac{S_p}{S_p^0}), \tag{33}$$

where $S_p=\dfrac{\sigma_{pp}^{c}\mid_{R_p=R_p(0)}}{\sigma_{pp}^{0}\mid_{R_p=R_p(0)}}$; $S_p^0=\lim\limits_{k\sigma\to 0}\dfrac{\sigma_{pp}^{c}\mid_{R_p=R_p(0)}}{\sigma_{pp}^{0}\mid_{R_p=R_p(0)}}$;

$\lim\limits_{k\sigma\to 0}\sigma_{pp}^0=A+B+C;\ p=h,v.$

S_p is the ratio of the complementary term to the total scattering coefficients. Terms A, B, and C represent Kirchhoff, cross, and complementary terms, respectively.

IV. NUMERICAL SIMULATION

Since the improved model is applicable to the small to moderate rough surface scattering problems, the surface parameters for numerical simulation should be selected on this condition. To evaluate the scattering coefficients efficiently, a single-scattering expression (19) is applied. The single scattering coefficients have been widely used for surface scattering and its early version was already demonstrated by Macelloni's experiments [9] with a frequency range of 2-18 GHz. Besides, according to Tang's [10] observation, the reflected energy for single scattering is about 95% of the total reflected energy for smooth surfaces with $\sigma/l<0.25$ (σ is RMS height, l is the correlation length) and is still dominant (~65%) for surfaces with an intermediate roughness $\sigma/l<0.5$. Thus, if the value of the $k\sigma$ is determined in the simulation, the parameter l is limited to a range that σ/l is smaller than 0.25. We adopt some typical soil permittivity in the numerical simulation. For a real case, in order to match the radar

data, some semi-empirical calibration methods for IEM were required. For example, Baghdadi, et al. [11], replaced the measured correlation length by a calibration parameter corresponding to optimal correlation length, so that model simulations would closely agree with radar measurements. However, this is not what we consider here. In this section, the improved IEM2Mc was compared with the SPM, KA and MoM for rough surfaces in mono- and bistatic observation.

Figure 1 shows bistatic scattering coefficients calculated by four models for Gaussian rough surface ($k\sigma$ = 0.1, kl = 1.5) in small RMS height region. The incidence angle and scattering angle are θ_i = 30°, ϕ_i = 0°, ϕ_s = 30°. The simulating codes are programmed in Matlab and are implemented on a personal computer with an AMD Athlon II 3 GHz processor. The computation time of the original IEM2Mc and the improved IEM2Mc is 32.72 s and 32.92 s, respectively. Therefore, the computation efficiency of the improved IEM2Mc is almost the same as the original IEM2Mc. From the Fig. 1, when the scattering angle θ is larger than 60°, the bistatic scattering coefficients which are computed by SPM and original IEM2Mc drop much more quickly than those of the AIEM and improved IEM2Mc. The improved IEM2Mc are much closer to the AIEM.

Figure 2 is the comparing result in KA region with simulation parameters: f = 5 GHz, $k\sigma$ = 0.84, kl = 12.56, ε_r = 5.5+i2.2, θ_i = 40°, ϕ_i = 0°, ϕ_s = 0°, 180°. According to Fig. 2, the difference between the improved IEM2Mc and the original IEM2Mc becomes obvious when the scattering angle is large. This phenomenon verifies the conclusion by Wu [7], that the sum of horizontal and vertical Fresnel reflection coefficients is important for bistatic scattering when an accurate prediction is required. When the RMS height increases, Kirchhoff term will contribute more in the surface current expressions. Therefore, the improved IEM2Mc has a good agreement with KA in Fig. 2. In Fig. 3, the improved IEM2Mc is compared with the MoM [12] with $k\sigma$ = 1 and kl = 6. It shows that the bistatic scattering coefficients calculated by the improved IEM2Mc are closer to those by the MoM than the original IEM2Mc.

Next, we check the backscattering results between the improved IEM2Mc and the original IEM2Mc in Fig. 4. The MoM data is from Du [13]. The improved IEM2Mc agrees well with the MoM data than the original IEM2Mc, especially when the observation angle is large. However, both the original and improved IEM2Mc fail to match well with MoM at small angles of incidence.

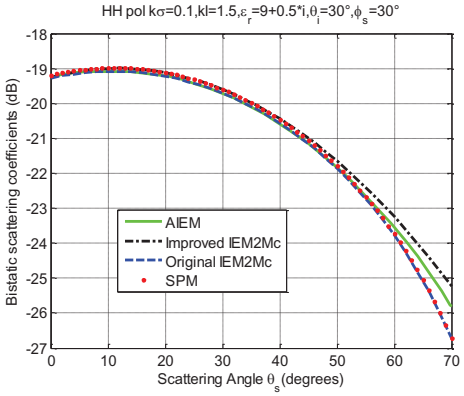

(a)

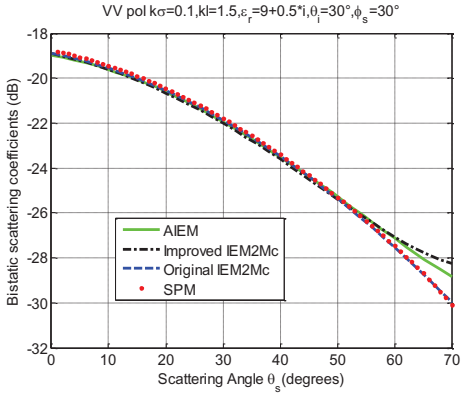

(b)

Fig. 1. The bistatic scattering coefficients obtained with SPM, the original IEM2Mc and the improved IEM2Mc at θ_i = 30°, ϕ_i = 0°, ϕ_s = 30°, with rough surface $k\sigma$ = 0.1, kl = 1.5: (a) co-polar horizontal polarization, and (b) co-polar vertical polarization.

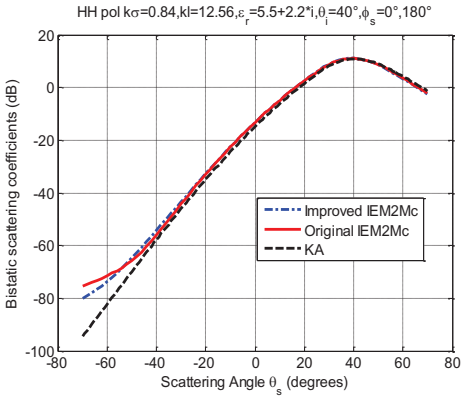

(a)

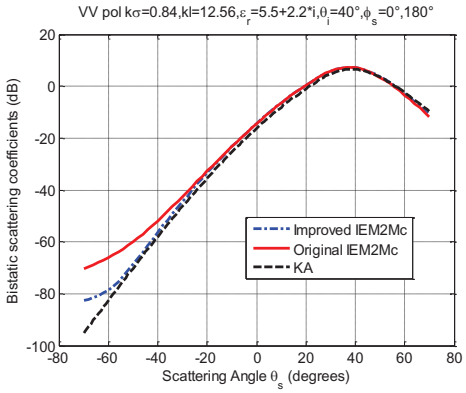

(b)

Fig. 2. Comparison of the bistatic scattering coefficients predicated by KA, the original IEM2Mc and the improved IEM2Mc at 5 GHz: (a) $\theta_i = 40°$ and co-polar horizontal polarization, and (b) $\theta_i = 40°$ and co-polar vertical polarization.

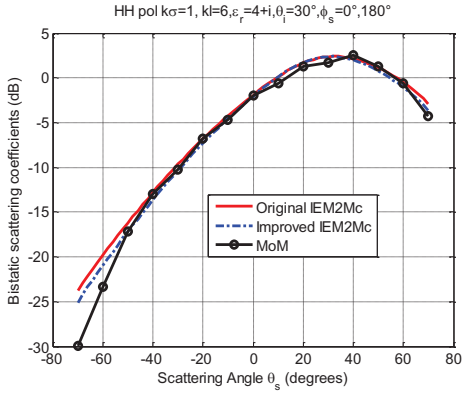

(a)

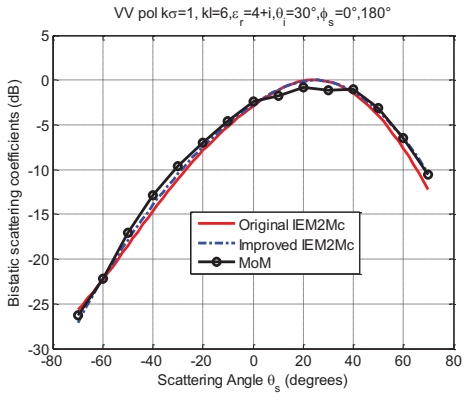

(b)

Fig. 3. Comparison of the bistatic scattering coefficients predicated by MoM, the original IEM2Mc and the improved IEM2Mc: (a) $\theta_i = 30°$ and co-polar horizontal polarization, and (b) $\theta_i = 30°$ and co-polar vertical polarization.

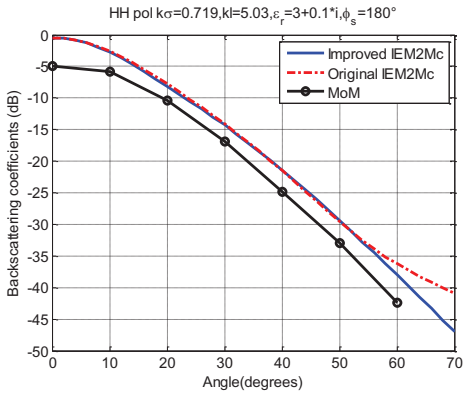

(a)

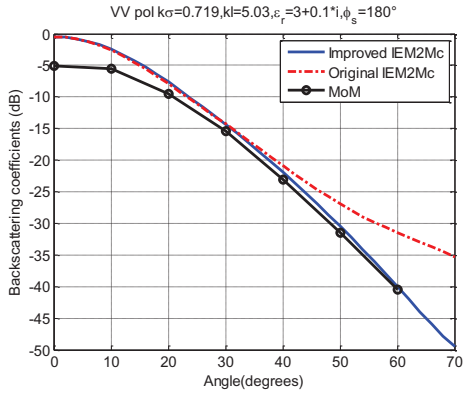

(b)

Fig. 4. The backscattering scattering coefficients obtained with MoM, the original IEM2Mc and the improved IEM2Mc with rough surface: (a) $k\sigma = 0.719$, $kl = 5.03$ and co-polar horizontal polarization, and (b) $k\sigma = 0.719$, $kl = 5.03$ and co-polar vertical polarization.

V. CONCLUSION

In this paper, an improved IEM2Mc model for surface bistatic scattering is derived with small or moderated RMS height. The full forms of the surface current terms in the Kirchhoff surface fields are reserved, so that the bistatic scattering coefficients are more accurate and more general. Besides, the physical-based approach with transition function to predict the Fresnel coefficients is proved to be better in the improved IEM2Mc than the posteriori method. The simulating results indicate that the improved IEM2Mc has better prediction than the original IEM2Mc, when comparing with SPM, KA, and MoM.

ACKNOWLEDGMENT

This work was supported in part by the National Natural Science Foundation of China under Grant

41176156, 41275032, and 61201123.

REFERENCES

[1] A. K. Fung, Z. Li, and K. S. Chen, "Backscattering from a randomly rough dielectric surface," *IEEE Trans. Geosci. Remote Sens*., vol. 30, no. 2, pp. 356-369, Mar. 1992.

[2] C. Y. Hsieh, A. K. Fung, G. Nesti, A. J. Sieber, and P. Coppo, "A further study of the IEM surface scattering model," *IEEE Trans. Geosci. Remote Sens*., vol. 35, no. 4, pp. 901-909, Jul. 1997.

[3] J. Alvarez-Perez, "An extension of the IEM/ IEMM surface scattering model," *Waves Random Media*, vol. 11, no. 3, pp. 307-329, Mar. 2001.

[4] K. S. Chen, T. D. Wu, L. Tsang, Q. Li, J. C. Shi, and A. K. Fung, "Emission of rough surfaces calculated by the integral equation method with comparison to three-dimensional moment method simulations," *IEEE Trans. Geosci. Remote Sens*., vol. 41, no. 1, pp. 90-101, Jan. 2003.

[5] Y. Du, "A new bistatic model for electromagnetic scattering from randomly rough surfaces," *Waves Random Media*, vol. 18, no. 1, pp. 109-128, Feb. 2008.

[6] J. Alvarez-Perez, "The IEM2M rough-surface scattering model for complex-permittivity scattering media," *Waves Random Media*, vol. 22, no. 2, pp. 207-233, May 2012.

[7] T. D. Wu, K. S. Chen, J. Shi, H. W. Lee, and A. K. Fung, "A study of an AIEM model for bistatic scattering from randomly rough surfaces," *IEEE Trans. Geosci. Remote Sens*., vol. 45, no. 9, pp. 2584-2598, Sep. 2008.

[8] T. D. Wu, K. S. Chen, J. Shi, and A. K. Fung, "A transition model for the reflection coefficient in surface scattering," *IEEE Trans. Geosci. Remote Sens*., vol. 39, no. 9, pp. 2040-2050, Sep. 2001.

[9] G. Macelloni, G. Nesti, P. Pampaloni, S. Sigismondi, D. Tarchi, and S. Lolli, "Experimental validation of surface scattering and emission models," *IEEE Trans. Geosci. Remote Sens*., vol. 38, no. 1, pp. 459-469, Jan. 2000.

[10] K. Tang and R. O. Buckius, "A statistical model of wave scattering from random rough surfaces," *International Journal of Heat and Mass Transfer*, vol. 44, pp. 4059-4073, 2001.

[11] N. Baghdadi, I. Gherboudj, M. Zribi, M. Sahebi, C. King, and F. Bonn, "Semi-empirical calibration of the IEM backscattering model using radar images and moisture and roughness field measurements," *International Journal of Remote Sens*., vol. 25, no. 18, pp. 3593-3623, Sep. 2004.

[12] F. Demontoux, C. Duffour, Y. Kerr, L. Kosolapova, H. Lawrence, V. Mironov, and J. P. Wigneron, "Coupling the temperature and mineralogy dependable soil dielectric model and a numerical model to compute scattering coefficient of complex multilayer soil structures," in *Proceedings of the Symposium on Remote Sensing of Natural Covers by Synthetic Aperture Radars*, Ulan-Ude, Russian Federation, pp. 330-343, 2010.

[13] Y. Du, J. A. Kong, W. Yan, Z. Wang, and L. Peng, "A statistical integral equation model for shadow-corrected EM scattering from a Gaussian rough surface," *IEEE Trans. Antennas Propag*., vol. 55, no. 6, pp. 1843-1855, Jun. 2007.

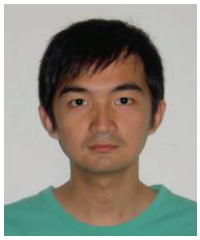

Wenchao Zheng received the B.S. degree in Electrical Engineering from Xi'an Institute of Posts and Telecommunications, Xi'an, China, in 2008 and the M.S. degree in Electrical Engineering from Wuhan Research Institute of Posts and Telecommunications, Wuhan, China in 2011.

He is currently pursuing the Ph.D. degree in Huazhong University of Science and Technology, Wuhan, China. His research interests include microwave remote sensing and multi-band antenna design.

Yi Leng (M'13) received the B.S. degree in Electronic Engineering from National University of Defense Technology, Changsha, China, in 1999, and the Ph.D. degree in Electronic Science and Technology from Huazhong University of Science and Technology, Wuhan, China, in 2008.

He is currently a Research Associate and Vice Director of Electromagnetic Engineering Research Center at Air Force Early Warning Academy, Wuhan, China. His current research interests include microwave antennas, wireless communication, and electromagnetic countermeasure.

Qingxia Li (M'08) received the B.S., M.S. and Ph.D. degrees in Electrical Engineering from Huazhong University of Science and Technology, Wuhan, China, in 1987, 1990, and 1999, respectively.

He is presently a Professor in Science and Technology on Multi-Spectral Information Processing Laboratory (School of Electronic Information and Communications), Huazhong University of Science and Technology,

Wuhan, China. His research interests include microwave remote sensing and deep space exploration, electromagnetic theory and application, antenna array and signal processing.